PAGEOPH, Vol. 144, Nos. 3/4 (1995) 0033-4553/95/040569-25$1.50 + 0.20/0

Laboratory Experiments of Tsunami Runup on a Circular Island

MICHAEL J. BRIGGS,[1] COSTAS E. SYNOLAKIS,[2] GORDON S. HARKINS,[1] and DEBRA R. GREEN[1]

Abstract—Laboratory experiments of a 7.2-m-diameter conical island were conducted to study three-dimensional tsunami runup. The 62.5-cm tall island had 1 on 4 side slopes and was positioned in the center of a 30-m-wide by 25-m-long flat-bottom basin. Solitary waves with height-to-depth ratios ranging from 0.05 to 0.20 and "source" lengths ranging from 0.30 to 7.14 island diameters were tested in water depths of 32 and 42 cm. Twenty-seven capacitance wave gages were used to measure surface wave elevations at incident and four radial transects on the island slope. Maximum vertical runup measurements were made at 20 locations around the perimeter of the island using rod and transit. A new runup gage was located on the back or lee side of the island to record runup time series.

Key words: Tsunamis, tsunami runup, laboratory experiments, physical models, three-dimensional models, tsunami simulation, solitary waves, wavemakers, tsunami evolution, instrumentation.

1. Introduction

Recently, tsunamis in Indonesia and Japan caused millions of dollars in damages and killed thousands of people. On December 12, 1992, a 7.5-magnitude earthquake off Flores Island, Indonesia, killed nearly 2,500 people and washed away entire villages (YEH *et al.*, 1993; 1994). Field surveys found an average runup height near Riangkrok of 19.6 m, with a maximum height of 26 m. Reflection off Flores Island may have been partially responsible for the catastrophe at Babi Island, where 750 people were killed due to tsunami waves running up to 7.3 m above SWL. On July 12, 1993, a magnitude 7.8 earthquake off Okushiri Island, Japan, triggered a devastating tsunami with recorded runup measurements as high as 30 m. This tsunami resulted in larger property damage than any 1992 tsunamis, and it completely inundated an entire village with overland flow. Property damage was $600 million.

When a tsunami approaches an island from deep water, it undergoes refraction, diffraction, breaking, and wave trapping. The tsunami increases in height and

[1] USAE Waterways Experiment Station, Coastal Engineering Research Center, Vicksburg, MS 39180-6199, U.S.A.

[2] Department of Civil and Aerospace Engineering, University of Southern California, Los Angeles, CA, U.S.A.

steepness with complicated currents and multiple wave trains. Edge waves may even develop depending on beach slope and bathymetry, coastline irregularity, and incident wave direction. Reflections from adjacent shorelines may affect the number of tsunami waves and their amplitudes around the perimeter of the island.

Several numerical models have been developed to solve the linear, mild-slope equations for regular periodic waves approaching a circular island (SMITH and SPRINKS, 1975; JONSSON and SKOVGAARD, 1979). However, none of these models calculate wave runup, which is the most devastating hazard associated with tsunamis. The only available experimental data on wave runup on a circular island were obtained by PROVIS (1975). His conical island had a diameter of 3 m and a slope of 1 on 10. It was positioned in a 5.55-m-wide and 5.80-m-long wave basin. The water depth was only 15 cm, which caused the data to be dominated by laboratory scale effects (SPRINKS and SMITH, 1983). They found that viscous damping and standing waves between the wavemaker and the island contaminated the experimental results.

Field surveys of tsunami damage on both Babi and Okushiri Islands showed unexpectedly large runup heights, especially on the back or lee side of the island. Interestingly, numerical simulations by different international teams of the wave runup for both tsunamis produced results which differed substantially from the field measurements, often by factors of ten. Recognizing the need for a better understanding of the important physical parameters involved in three-dimensional tsunami runup, the National Science Foundation funded a three-year study beginning in 1992. This joint research study includes participants from Cornell University, Harvard University, University of Washington, University of Southern California (USC), and the U.S. Army Engineer Waterways Experiment Station (WES).

One of the goals of this project is to develop large-scale experimental databases for verification and modification of numerical models. Previous laboratory studies focused on tsunami wave runup on a plane 1 on 30 beach (BRIGGS *et al.*, 1993). A conical island was selected for study because of its mathematical simplicity and realistic geometry to actual islands (i.e. Babi Island, Okushiri Island, Hawaiian Islands). These large-scale experiments were conducted at WES during 1993 and 1994.

LIU *et al.* (1994) obtained very good agreement between this experimental data and their nonlinear, shallow-water model with bottom friction for the free surface displacements and maximum runup heights. The numerical model uses a staggered explicit finite difference leapfrog scheme to solve the governing equations. The numerical model was then used to examine several other important processes including velocity field, wave trapping around the island, and beach slope effects on runup heights.

In this paper, results from the wave height evolution and runup measurements on the island are presented. First, the experimental design including the physical

model, wavemaker, and instrumentation are described. Next, a description of the tsunami wave simulation using solitary waves is given. Thereafter, amplitude evolution is briefly described. Finally, results from the measurements of maximum runup around the perimeter of the island and runup histories are presented and discussed.

2. Laboratory Experiments

2.1 Physical Model

A physical model of a conical island was constructed in the center of a 30-m-wide by 25-m-long flat-bottom basin at WES (Figure 1). The island had the shape of a truncated, right circular cone with diameters of 7.2 m at the toe and 2.2 m at the crest. The vertical height of the island was approximately 62.5 cm, with 1 V on 4 H beach face (i.e. $\beta = 14°$). The surface of the island and basin were constructed with smooth concrete. Tests were conducted at two water depths, 32 and 42 cm, to vary the relative waterline diameter of the island.

The X axis (X) of the right-hand, global coordinate system was perpendicular to the wavemaker and the Y axis (Y) was parallel to the wavemaker. The origin was

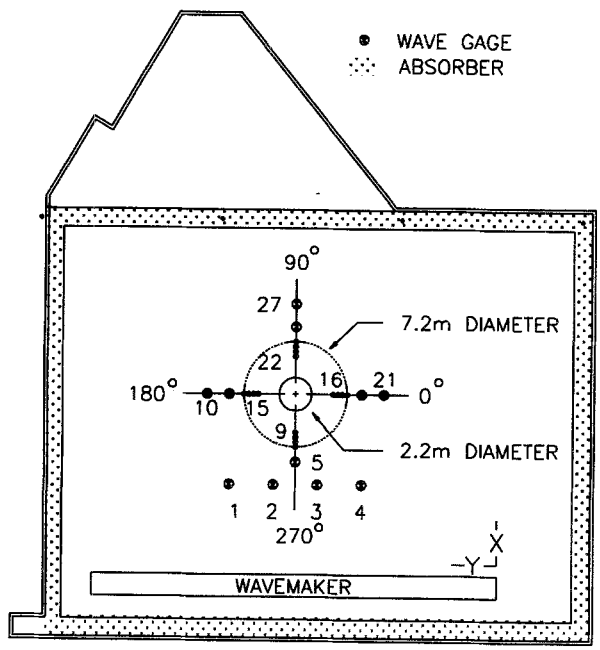

Figure 1
Schematic of island and wave gages.

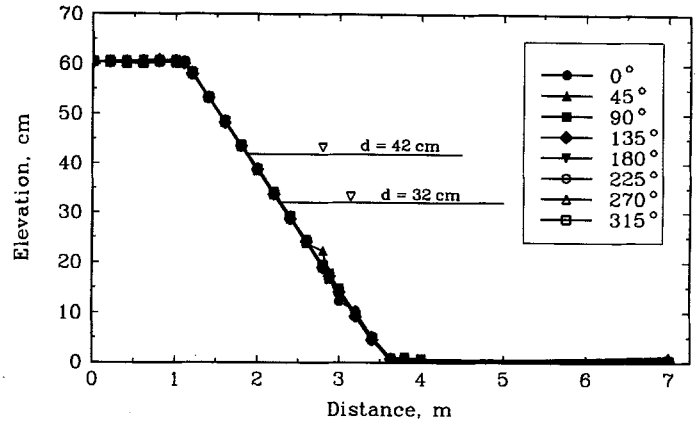

Figure 2
Circular island bathymetry for eight radial transects.

located at the end of the wavemaker, in line with the front surface of all paddles at their rest position. The center of the island was located at $X = 12.96$ m and $Y = 13.80$ m. A local coordinate system (x, y) was located at the center of the island. Angles increase counterclockwise (polar convention) from the x axis (x) pointing in the 0° direction (see Figure 1).

Bathymetric surveys of the island at eight radial transects showed it to be very uniform (Figure 2). The largest variation was a slight "bump" on the 45° transect at an elevation of approximately 22 cm. A bathymetric survey of the basin revealed a maximum elevation of 2.8 cm, a minimum of -1.4 cm, and a standard deviation of 7.3 mm. The basin sides and rear were lined with wave absorber to minimize wave reflections and cross-basin seiche. The irregular shape of the rear wall minimized reflections into the study area.

2.2 Wavemaker

A directional spectral wave generator (DSWG), designed and built by MTS Systems Corporation, was used to generate tsunami waves. Figure 3 shows a wave shoaling and refracting around the island with the DSWG in the background. The electronically controlled DSWG is 27.4-m-long and consists of 60 paddles, 46 cm wide and 76 cm high. The paddles are grouped in four modules of 15 paddles. Each of the 61 paddle joints is independently driven in piston mode by a 3/4-HP closed-loop dc servometer. The paddles are connected in a continuous chain with flexible polyethylene seals to produce smooth wave forms using the "snake principle" without spurious waves from end effects. Maximum stroke of the DSWG is 30.5 cm.

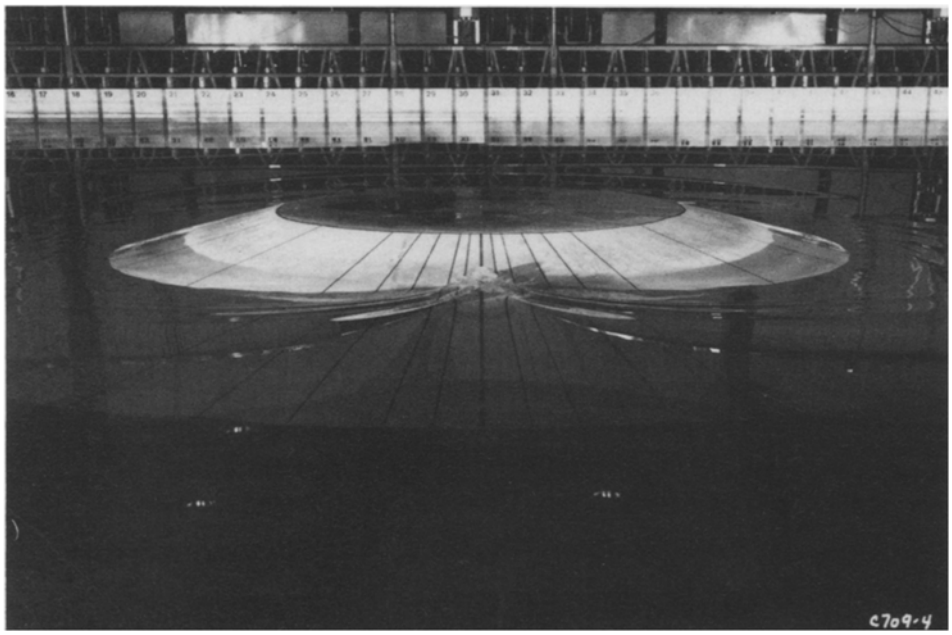

Figure 3
Overhead photograph showing runup around island.

Digital and analog circuits comprising the DSWG control console were located in a nearby climate-controlled room. This MTS console supplies digital wave-board control signals for input to 61 Preston digital-to-analog (D/A) signal converters. Minicomputers (a) perform D/A conversion for the 61 paddles at run time, (b) monitor paddle displacement and feedback, (c) calibrate wave gages, (d) digitize data, (e) update the control signals, and (f) analyze collected data (BRIGGS and HAMPTON, 1987).

2.3 Instrumentation

Twenty-seven capacitance wave gages were used to measure surface wave elevations (see Figure 1). The first four gages were located parallel to the wave-maker to measure incident wave conditions. Prior to each run, these gages were moved seaward from the toe of the island a distance equivalent to half-a-wave-length (i.e. L/2) of the wave to be generated. This procedure insured that the tsunami wave was always measured at the same relative stage of evolution.

A circular measurement grid of six concentric circles covers the island to a distance 2.5 m beyond the toe. Measurement points were located at the intersection

of these concentric circles and the 90° radial lines. The spacing between the grid points was a function of the water depth. The shallowest gage was located in an 8-cm depth and the deepest gage was located over the toe. Two gages were evenly spaced between these points along each 90° transect. Two additional gages were spaced in the deepwater portion at distances of 1.0 m and 2.5 m from the toe (except for the 270° transect). Table 1 lists the X, Y, and Z coordinates for each of the 27 gages for both water depths.

A unique aspect of these tests was the measurement of runup time histories using a new digital runup gage (Figure 4). YEH *et al.* (1989) used a digital runup gage embedded in a model beach to study runup velocities of a bore propagating up the beach. His 35-cm-long gage consisted of 8 rods spaced 5 cm apart with tips which projected no more than 1 mm above the beach surface. The runup gage used in this study possesses some special features which were newly developed. Rather

Table 1

Wave gage locations

Gage ID	*X*, *m*	*Y*, *m*	*Z* (cm)	Comments
		$d = 32$ cm		
1	$f(L/2)$	16.05	32.0	Incident gage
2	$f(L/2)$	14.55	32.0	Incident gage
3	$f(L/2)$	13.05	32.0	Incident gage
4	$f(L/2)$	11.55	32.0	Incident gage
5	8.36	13.80	32.0	270° transect
6	9.36	13.80	31.7	270° transect
7	9.76	13.80	22.5	270° transect
8	10.08	13.80	14.7	270° transect
9	10.36	13.80	8.2	270° transect
10	12.96	19.93	32.0	180° transect
11	12.96	18.43	32.0	180° transect
12	12.96	17.43	31.5	180° transect
13	12.96	17.00	22.5	180° transect
14	12.96	16.68	14.6	180° transect
15	12.96	16.40	7.9	180° transect
16	12.96	11.22	7.9	0° transect
17	12.96	10.92	15.2	0° transect
18	12.96	10.60	21.9	0° transect
19	12.96	10.25	30.1	0° transect
20	12.96	9.17	32.0	0° transect
21	12.96	7.67	32.0	0° transect
22	15.56	13.80	8.3	90° transect
23	15.84	13.80	15.7	90° transect
24	16.16	13.80	22.8	90° transect
25	16.59	13.80	31.7	90° transect
26	17.59	13.80	32.0	90° transect
27	19.09	13.80	32.0	90° transect

Table 1 (*Cont.*)

Gage ID	X, m	Y, m	Z (cm)	Comments
		$d = 42$ cm		
1	$f(L/2)$	16.05	42.0	Incident gage
2	$f(L/2)$	14.55	42.0	Incident gage
3	$f(L/2)$	13.05	4.20	Incident gage
4	$f(L/2)$	11.55	4.20	Incident gage
5	8.36	13.80	42.0	270° transect
6	9.36	13.80	42.0	270° transect
7	9.81	13.80	30.7	270° transect
8	10.27	13.80	19.3	270° transect
9	10.72	13.80	8.0	270° transect
10	12.96	19.93	42.0	180° transect
11	12.96	18.43	42.0	180° transect
12	12.96	17.43	42.0	180° transect
13	12.96	16.98	30.7	180° transect
14	12.96	16.52	19.3	180° transect
15	12.96	16.07	8.0	180° transect
16	12.96	11.53	8.0	0° transect
17	12.96	11.08	19.3	0° transect
18	12.96	10.62	30.7	0° transect
19	12.96	10.25	42.0	0° transect
20	12.96	9.17	42.0	0° transect
21	12.96	7.67	42.0	0° transect
22	15.20	13.80	8.0	90° transect
23	15.65	13.80	19.3	90° transect
24	16.11	13.80	30.7	90° transect
25	16.59	13.80	42.0	90° transect
26	17.59	13.80	42.0	90° transect
27	19.09	13.80	42.0	90° transect

than a continuous wire or rod placed along the bottom, this new prototype gage consisted of a series of 32 surface-piercing, vertical rods which are turned on or off by water contact. Gage resolution is limited by the 1-cm minimum spacing between rods. Software is used to convert the wetted rod number to the appropriate vertical runup or rundown. The gage is positioned along the transect so that the still-water level is approximately midway among the rods, enabling measurement of runup and rundown. The advantage of this design is that runup can be measured in the laboratory for uneven bottom conditions, such as rubble-mound breakwaters. For these tests, the runup gage was located only at the 90° transect on the back or lee side of the island. Based on the success of these tests, four new runup gages with 64 rods were designed. They will be used in future tests to cover each of the 90° transects (i.e., 0°, 90°, 180°, and 270°) around the perimeter of the island.

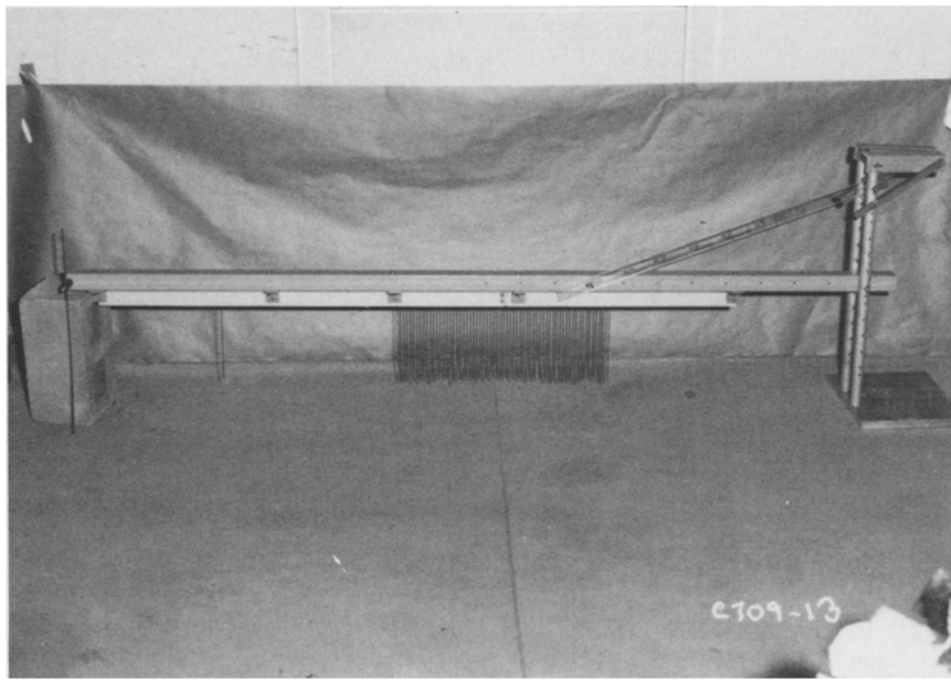

Figure 4
Prototype runup gage.

3. Tsunami Wave Simulation

3.1 Solitary Waves

Tsunami waves were simulated using solitary waves because they model some of the coastal effects of tsunamis well. Although the solitary wave is a single wave, it consists of a complex spectrum of frequencies that allows for elegant analysis and reliable generation in the laboratory. Also, it propagates over constant depth without appreciable changes, allowing for consistent referencing of its offshore or incident wave height. SYNOLAKIS (1987) and others have used the height-to-depth ratio $\mathbf{H} = H/d$ to describe solitary waves. The surface profile $\eta(x, t)$ for a wave centered at $x = X_1$ and time $t = 0$ is defined as

$$\eta(x, 0) = \mathbf{H} \operatorname{sech}^2 \gamma(x - X_1) \tag{1}$$

where $\gamma = (0.75\,\mathbf{H})^{1/2}$. A measure of the wavelength L can be defined in terms of $\mathbf{H}$ and water depth d as

$$L = \frac{2d}{\gamma} \operatorname{arccosh} \sqrt{20} \tag{2}$$

so that it is equal to the distance between the two end points in the symmetric profile where the height is 5 percent of the height at the crest H.

3.2 Target Parameters

Table 2 lists the target solitary wave parameters for the different **H** values used for each water depth. Due to stroke limitations of the DSWG, a maximum $\mathbf{H} = 0.20$ was used for these tests. Because of the flat offshore region and relatively steep island slopes, these waves were nonbreaking until final stages of transformation near the shoreline where gentle spilling occurred.

As mentioned previously, two water depths ($d = 32$ and 42 cm) were used to change the effective island diameter D and beach exposed to the tsunami wave runup. Different DSWG lengths S (i.e., number of paddles) were used to vary the source length of the incoming tsunami wave. Both symmetric and eccentric source lengths were investigated. Symmetric cases were centered about the center of the DSWG and eccentric cases were offset from the center of the island a distance D_x along the x-axis and D_y along the y axis (i.e., waves were not generated directly at the island). Corresponding dimensionless parameters $\mathbf{S_D}(=S/D)$, $\mathbf{D}_x(=D_x/d)$, and $\mathbf{D}_y(=D_y/d)$ are listed in Table 3 for the different symmetric and eccentric cases as a function of the number of modules m and their associated paddle locations. Not all cases were run for each **H**.

The solitary wave control signal was imbedded in a longer control signal, which included a long ramp time and wait time before and after the main solitary wave to allow the water to still. Since solitary waves are generated with a single positive stroke, the wavemaker was ramped back to its minimum excursion (i.e., largest negative stroke) to enable use of its full stroke capability. The entire control signal was converted to an analog signal with a D/A rate of 20 Hz.

Table 2

Target solitary wave parameters

No.	H	Height (cm)	Length (m)	Period (sec)
		$d = 32$ cm		
1	0.05	1.60	7.20	7.01
2	0.10	3.20	5.09	4.90
3	0.20	6.40	3.60	3.41
		$d = 42$ cm		
4	0.05	2.10	9.46	8.03
5	0.08	3.36	7.48	6.31
6	0.10	4.20	6.69	5.62

Table 3

Dimensionless wavemaker lengths

m	Description	No. Paddles	Paddle ID From	Paddle ID To	S (cm)	S_D $d=32$	S_D $d=42$	D_x $d=32$	D_x $d=42$	D_y $d=32$	D_y $d=42$
					Symmetric Cases						
0.25	1/4 Module Center	4	29	32	137.2	0.30	0.36	40.50	30.86	0.0	0.0
0.5	1/2 Module Center	8	27	34	320.0	0.69	0.83	40.50	30.86	0.0	0.0
1	1 Module Center	15	24	38	640.1	1.38	1.67	40.50	30.86	0.0	0.0
1.5	1.5 Module Center	23	19	42	1005.8	2.17	2.62	40.50	30.86	0.0	0.0
2	2 Module Center	30	16	45	1325.9	2.86	3.45	40.50	30.86	0.0	0.0
3	3 Module Center	45	8	52	2011.7	4.34	5.24	40.50	30.86	0.0	0.0
4	4 Module Center	61	1	61	2743.2	5.91	7.14	40.50	30.86	0.0	0.0
					Eccentric Cases						
0.25*e*	1/4 Module End	4	1	4	137.2	0.30	0.36	40.50	30.86	40.7	31.0
0.5*e*	1/2 Module End	8	1	8	320.0	0.69	0.83	40.50	30.86	37.9	28.8
1*e*	1 Module End	16	1	16	685.8	1.48	1.79	40.50	30.86	32.1	24.5
2*e*	2 Module End	31	1	31	1371.6	2.96	3.57	40.50	30.86	21.4	16.3

Notes:

1. Island diameter at toe, cm = 720 cm
2. Island diameter at $d = 32$ cm waterline = 464 cm
3. Island diameter at $d = 42$ cm waterline = 384 cm

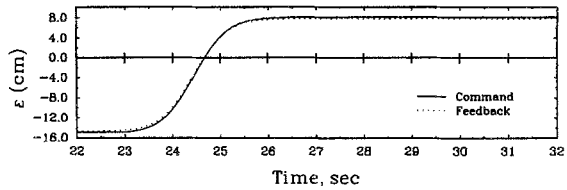

(a) Command and feedback control signal.

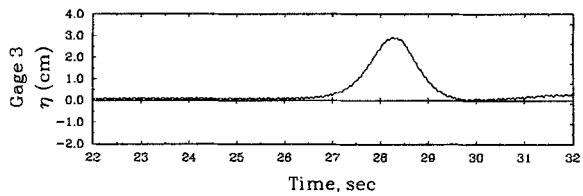

(b) Measured surface elevation for gage 3.

Figure 5
Surface elevation time series for $\mathbf{H} = 0.10$ at $d = 32$ for $m = 4$.

As an example, the top panel of Figure 5 shows the command and feedback control signal at the DSWG and the bottom panel shows the surface elevation for incident gage 3 for the target $\mathbf{H}_{tgt} = 0.10$, $m = 4$ modules, $d = 32$ cm condition in the basin. All data were collected at a sampling frequency $f_s = 25$ Hz. The command and feedback signals are nearly identical. The incident solitary wave profile is relatively clean, without spurious harmonics. Other cases manifested similar patterns. This information is important for future numerical model simulations/verifications of this laboratory data.

3.3 Measured Wave Heights

The shelf width is the distance (i.e., 9.36 m) between the DSWG and the toe of the island. For source lengths smaller than this value (i.e., less than $m = 1.5$ modules), the wave front is not uniform in the longshore direction due to radiation from the ends before it reaches the island. The incident wave front was very uniform when larger source lengths were used, however.

Measured wave heights are listed in Table 4 for each of the different cases at the two water depths. Both symmetric and eccentric source length cases are given for each target $\mathbf{H}$. The measured wave heights are an average of incident gages 2 and 3 (see Figure 1) for all runs for each case. Also listed are $\mathbf{H}_{meas}$ and the ratio of measured to target wave height $\mathbf{H}_{meas}/\mathbf{H}_{tgt}$.

In general, measured wave heights were smaller than target wave heights. For the symmetric cases when two or more modules were used, the measured wave height was approximatley 90 percent of the target value. The decrease in measured wave height from the target was due to losses in the mechanical generation of the solitary waves resulting from gaps between the floor and the wavemaker. For the smaller source lengths less than $m = 1.5$, the radiation condition from the end of the wave was an important factor in decreasing measured wave height. For $m = 1$, the average measured wave was only 60 percent of the target value. For $m = 0.25$ and 0.50, the measured wave heights were proportionally smaller.

For the eccentric cases ($m = 0.25e$ to $2e$), listed values reflect the fact that the incident gages were offset from the source. These small values indicate the size wave experienced by the island as opposed to the size wave actually generated. Actual measured values would have been the same as the corresponding symmetric case if

Table 4

Measured wave heights

		Wave Height, cm			
H	m	Target	Meas	$\mathbf{H}_{meas}$	$\mathbf{H}_{meas}/\mathbf{H}_{tgt}$
		$d = 32$ cm			
0.05	0.25	1.6	—	—	—
	0.5	1.6	—	—	—
	1	1.6	0.98	0.03	0.61
	1.5	1.6	—	—	—
	2	1.6	1.42	0.04	0.89
	3	1.6	1.47	0.05	0.92
	4	1.6	1.44	0.05	0.90
	1	1.6	—	—	—
	2	1.6	—	—	—
0.10	0.25	3.2	0.55	0.02	0.17
	0.5	3.2	1.07	0.03	0.34
	1	3.2	1.92	0.06	0.60
	1.5	3.2	—	—	—
	2	3.2	2.74	0.09	0.86
	3	3.2	2.82	0.09	0.88
	4	3.2	2.90	0.09	0.90
	1	3.2	0.63	0.02	0.20
	2	3.2	—	—	—
0.20	0.25	6.4	1.02	0.03	0.16
	0.5	6.4	2.13	0.07	0.33
	1	6.4	3.92	0.12	0.61
	1.5	6.4	—	—	—
	2	6.4	5.68	0.18	0.91
	3	6.4	5.81	0.18	0.90
	4	6.4	5.78	0.18	0.90
	1	6.4	1.10	0.03	0.17
	2	6.4	3.03	0.09	0.47

Table 4 (*Cont.*)

H	m	Wave Height, cm Target	Meas	H_{meas}	H_{meas}/H_{tgt}
			$d = 42$ cm		
0.05	0.25	2.1	0.37	0.01	0.17
	0.5	2.1	0.75	0.02	0.36
	1	2.1	1.28	0.03	0.61
	1.5	2.1	—	—	—
	2	2.1	1.83	0.04	0.87
	3	2.1	1.91	0.05	0.91
	4	2.1	1.91	0.05	0.91
	1	2.1	0.46	0.01	0.22
	2	2.1	0.47	0.01	0.22
0.08	0.25	3.4	0.53	0.05	0.59
	0.5	3.4	1.10	0.03	0.33
	1	3.4	2.00	0.05	0.59
	1.5	3.4	—	—	—
	2	3.4	2.92	0.07	0.87
	3	3.4	3.06	0.07	0.91
	4	3.4	3.07	0.07	0.91
	0.25	3.4	0.17	0.00	0.05
	0.5	3.4	0.37	0.01	0.11
	1	3.4	0.70	0.02	0.21
	2	3.4	1.62	0.04	0.48
0.10	0.25	4.2	0.70	0.02	0.17
	0.5	4.2	1.37	0.03	0.33
	1	4.2	2.41	0.06	0.57
	1.5	4.2	—	—	—
	2	4.2	3.66	0.09	0.87
	3	4.2	3.82	0.09	0.91
	4	4.2	3.83	0.09	0.91
	0.25	4.2	0.27	0.01	0.07
	0.5	4.2	0.55	0.01	0.13
	1	4.2	0.94	0.02	0.22
	2	4.2	—	—	—

the incident gages had been located symmetrically with the source. Shorter and longer eccentric source lengths were proportionately smaller or larger than their symmetric counterparts.

4. *Amplitude Evolution*

When tsunami waves approach the island they undergo complicated nonlinear transformations. Amplitude evolution for the four radial transects is shown in

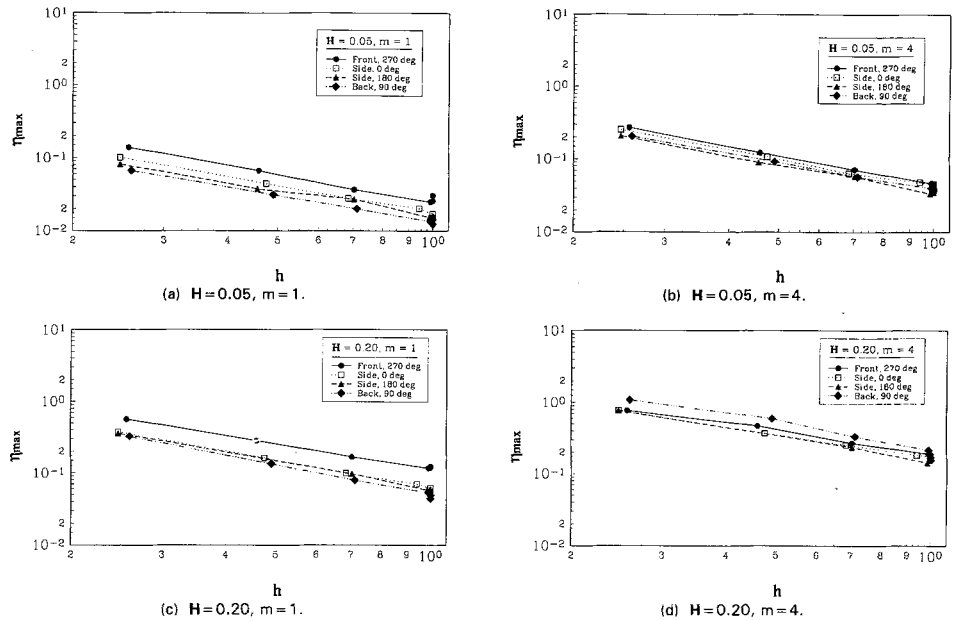

Figure 6
Normalized wave height evolution versus local water depth for $\mathbf{H} = 0.05$ and 0.20, $m = 1$ and 4, $d = 32$ cm.

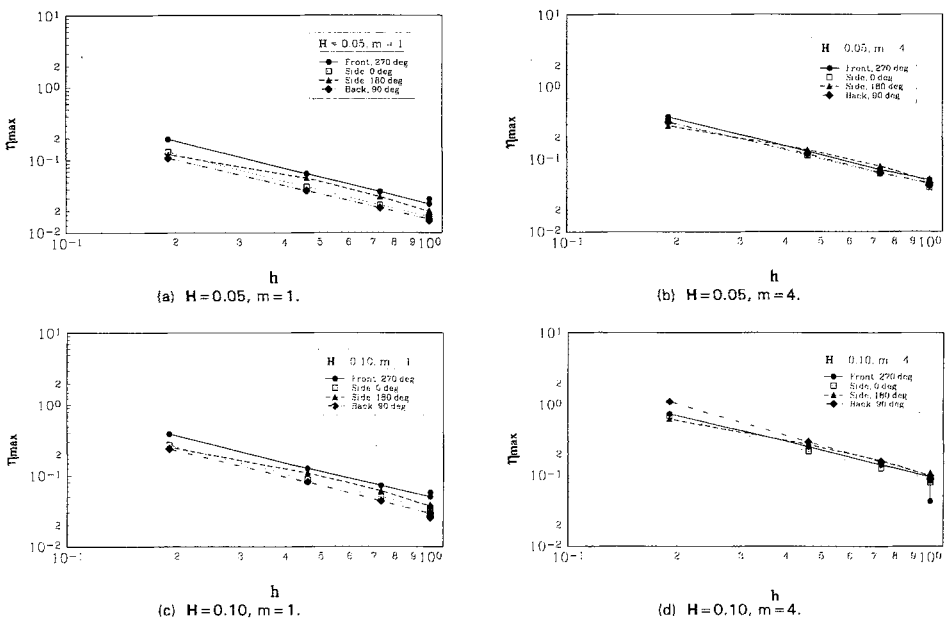

Figure 7
Normalized wave height evolution versus local water depth for $\mathbf{H} = 0.05$ and 0.10, $m = 1$ and 4, $d = 42$ cm.

Figure 6 for $d = 32$ cm for $\mathbf{H} = 0.05$ and 0.20 and $m = 1$ and 4 modules. The corresponding amplitude evolution with cross-shore distance for the deeper $d = 42$ cm cases is shown in Figure 7 for $\mathbf{H} = 0.05$ and 0.10. Dimensionless η_{max} (wave height at each gage η_{max} in the cross-shore radial transect normalized by the undisturbed water depth h at that gage) was plotted versus dimensionless gage depth $\mathbf{h}$ ($=h/d$).

In Figure 6a, the largest wave heights are on the front side of the island and the smallest are on the back side. For the larger source length of $m = 4$ in Figure 6b, there is a slight difference among the four transects in wave height, although the front side remains largest. For the larger $\mathbf{H} = 0.20$ in Figure 6c, the front side waves are still noticeably larger than the back side waves. However, for $m = 4$ in Figure 6d, the back side waves are larger because of the constructive effects of the edge waves. The same phenomenon occurs for the deeper depth cases in Figure 7.

5. Runup Measurements

In this section, results from maximum vertical runup measurements with a rod and transit and runup time series with the prototype runup gage are presented and discussed.

5.1 Maximum Vertical Runup Heights

Maximum vertical runup R_v was measured at twenty locations around the perimeter of the island. Sixteen were evenly spaced every 22.5° around the perimeter. Four radial transects with uneven spacing were located on the back side of the island (i.e., 90°) to improve the resolution in this critical area. At the conclusion of each run, maximum runup along each transect was manually located. A surveyor's rod and transit were then used to measure vertical runup at each transect.

Changes in runup shape and magnitude R were investigated by varying the water depth, wave height, source length (number of modules), and eccentricity of the source. Figures 8a–d are polar plots of maximum vertical runup for $d = 32$ cm, $\mathbf{H} = 0.05$ and 0.20 for $m = 1$ and 4 modules, respectively. Figures 9a–d are analogous plots for the deeper water $d = 42$ cm cases for $\mathbf{H} = 0.05$ and 0.10 for $m = 1$ and 4 modules, respectively. The tsunami wave propagated from the bottom in each panel of the figure. The island crest, waterline, and toe are shown for reference. Two or three runs of each case are overlain, demonstrating excellent repeatability.

In Figure 8a for $\mathbf{H} = 0.05$ and $m = 1$, runup is fairly uniform around the perimeter of the island. In Figure 8b for $m = 4$ modules and the same wave height, runup is higher on the front side. For the larger $\mathbf{H} = 0.20$ and $m = 1$ in Figure 8c, runup is still larger on the front side of the island; however, a distinctive pattern of

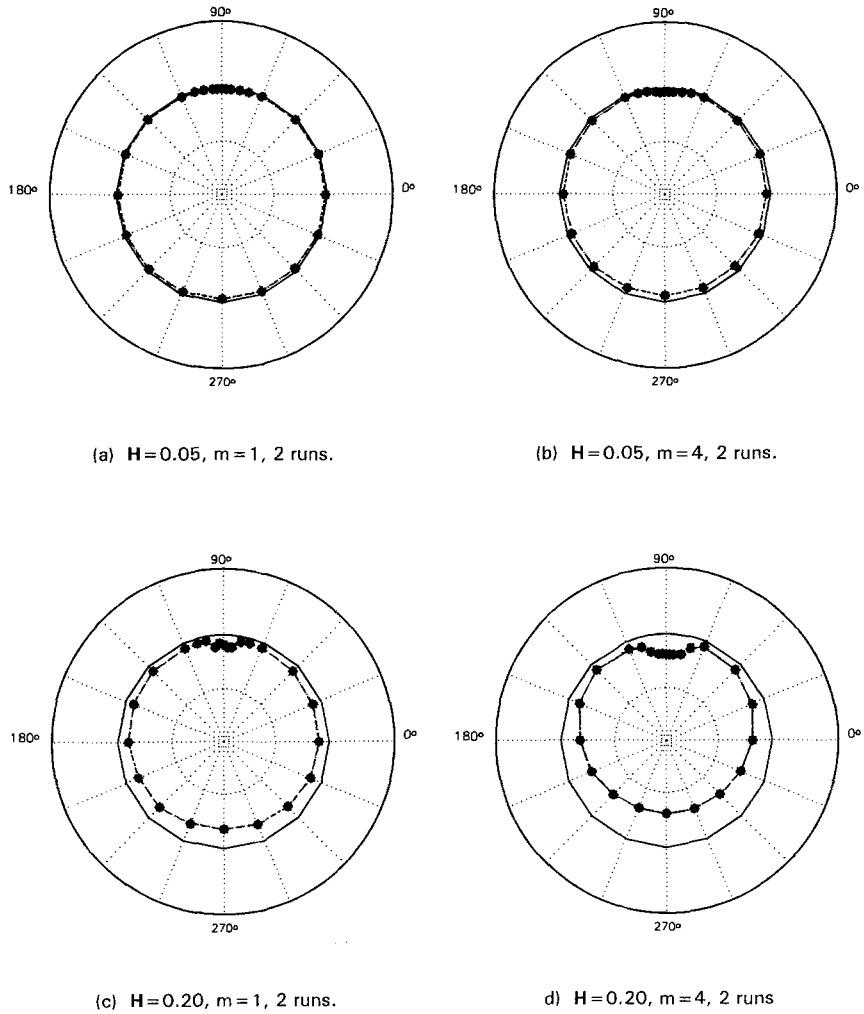

Figure 8
Maximum runup measurements for $\mathbf{H} = 0.05$ and 0.20, $m = 1$ and 4, $d = 32$ cm.

runup due to the edge waves propagating around the island from the symmetric source begins to become apparent. By Figure 8d for $m = 4$ modules, the runup on the back side is almost as large as that on the front side of the island. Similar patterns are suggested by Figure 9, except that runup on the back side is more pronounced. For $\mathbf{H} = 0.10$ and $m = 4$ in Figure 9d, runup on the back side is slightly larger than that on the front side. Refraction and diffraction cause the wave to bend around the island as edge waves. Because the island and source were symmetric, the wave wraps evenly around the island and produces relatively large runup on the back side. This is a very interesting phenomenon since most people

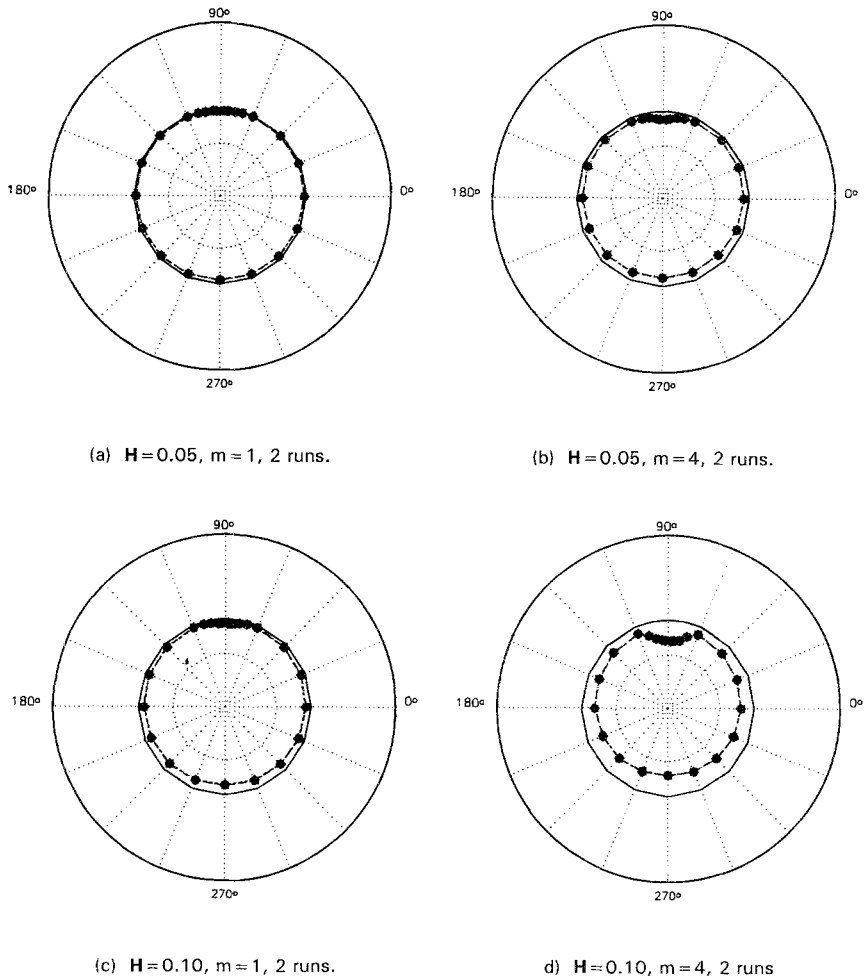

Figure 9
Maximum runup measurements for $\mathbf{H} = 0.05$ and 0.10, $m = 1$ and 4, $d = 42$ cm.

would feel "safe" on the back side of an island. When the source is offset from the island center (i.e., eccentricity effects), runup is largest on the island quadrant closest to the source between 0° and 270°, decreasing linearly around the perimeter to the opposite side. Figures 10a–d illustrate this effect for both water depths for the largest wave height of $\mathbf{H} = 0.20$ and 0.10 for $m = 1e$ and $2e$, respectively.

5.2 Maximum Runup versus Source Length

Maximum runup $\mathbf{R}$ versus length $\mathbf{S_D}$ values on the front, side and back of the island for the two water depths are shown in Figure 11. Values for the side of the

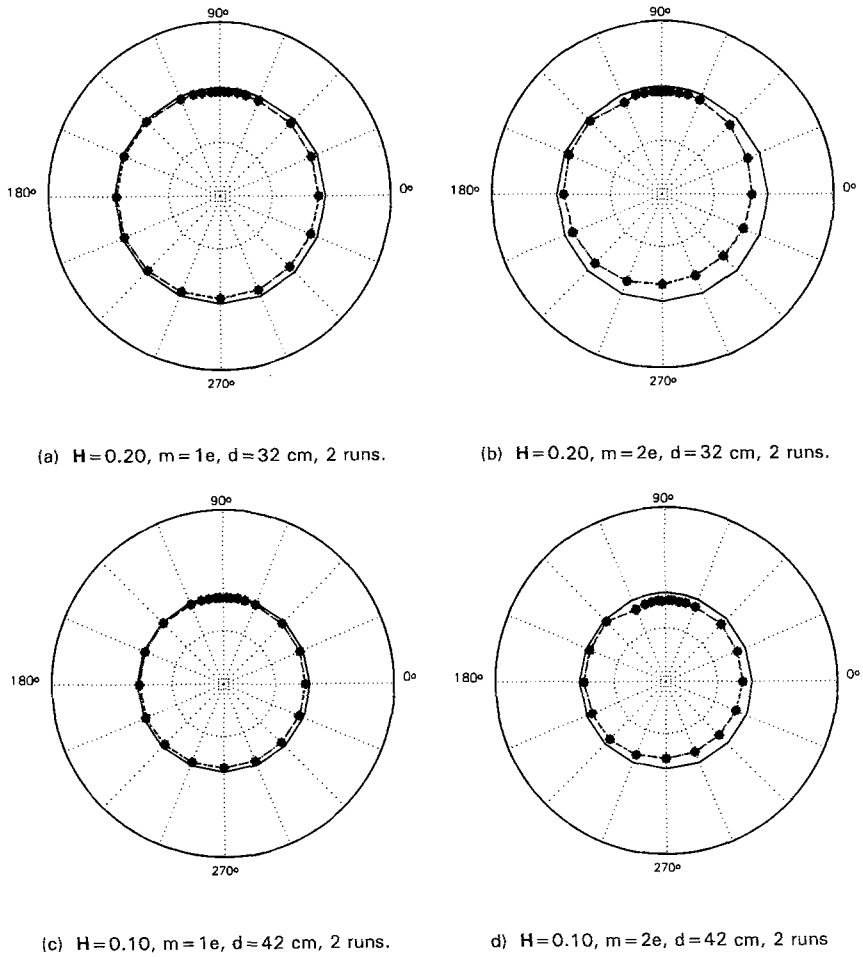

Figure 10
Maximum runup measurements for eccentric source, $\mathbf{H} = 0.20$ and 0.10, $m = 4$, $d = 32$, 42 cm.

island are an average from both 0° and 180° sides. Because the prototype runup gage was located on the back side of the island on the 90° transect for $d = 42$ cm, no values were collected. Least-square fit lines for each of the three target normalized wave height **H** values are also shown. A second order polynomial fit produced the highest correlation coefficient r^2 (i.e., best fit) for all cases. Quadratic equation coefficients a, b, and c corresponding to an equation of the form

$$\mathbf{R} = a + b\mathbf{S_D} + c\mathbf{S_D^2} \tag{3}$$

and the associated r^2 are listed in Table 5 for both the 32-cm and 42-cm water depths. These empirical equations can be used to estimate the runup on an island

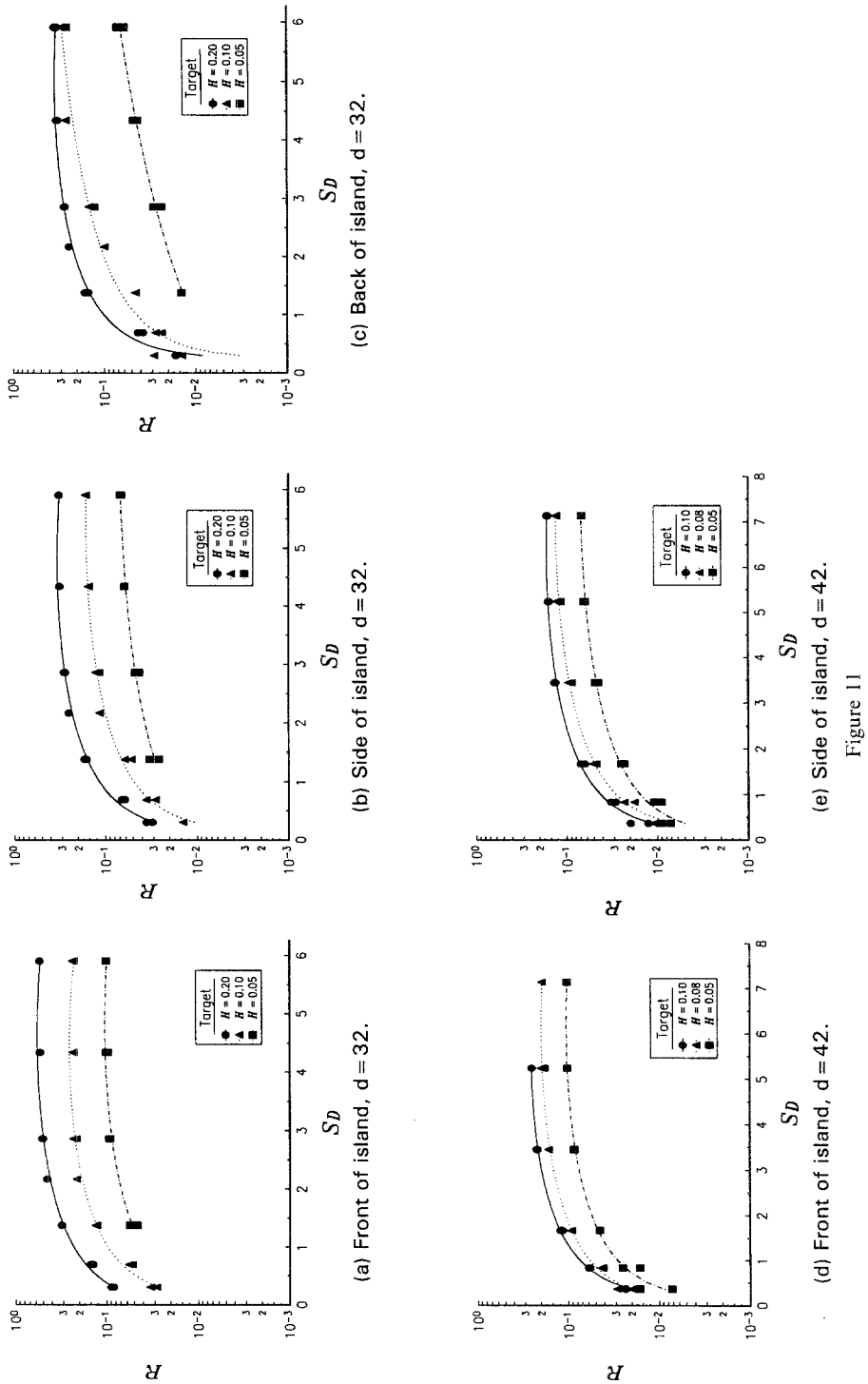

Figure 11
Maximum runup around island as a function of source length for two water depths.

Table 5

Least square parameters for R vs S_D

H	a	b	c	r^2
		Front, $d = 32$ cm		
0.20	0.0125	0.2444	−0.0264	0.99
0.10	−0.0079	0.1192	−0.0134	0.98
0.05	0.0031	0.0421	−0.0044	0.95
		Side, $d = 32$ cm		
0.20	−0.0137	0.1463	−0.0152	0.99
0.10	−0.0072	0.0620	−0.0056	0.99
0.05	−0.0079	0.0170	−0.0011	0.97
		Back, $d = 32$ cm		
0.20	−0.0358	0.1526	−0.0152	0.99
0.10	−0.0147	0.0608	−0.0016	0.96
0.05	0.0045	0.0057	0.0008	0.97
		Front, $d = 42$ cm		
0.10	−0.0137	0.0972	−0.0088	1.00
0.08	−0.0020	0.0654	−0.0053	0.99
0.05	−0.0036	0.0352	−0.0028	0.99
		Side, $d = 42$ cm		
0.10	−0.0078	0.0548	−0.0043	0.99
0.08	−0.0070	0.0383	−0.0026	0.99
0.05	−0.0013	0.0180	−0.0011	0.99

for the range of conditions studied. However, given the small coefficient of the second-order term, it is conjectured that a linear relationship between runup and source length, analogous to that found by BRIGGS *et al.* (1993) for the plane beach, could be used without loss of accuracy for empirical predictions.

5.3 Runup Time History

Measurement of maximum runup is a labor-intensive effort which only gives one value of runup and no information about rundown. A runup time series showing both runup (positive values) and rundown (negative values) is a more useful measurement for verification of numerical models and prediction of subsequent runup waves due to bathymetry variations and reflections from adjacent shorelines. Measurements were only made at the 90° transect on the back side of the island for selected deeper water cases. As previously stated, future tests are planned at each 90° transect around the perimeter of the island with four new runup gages.

Figure 12 is an example runup time series for $\mathbf{H} = 0.10$ and $m = 1$ module. The first runup and rundown wave is usually the largest. The maximum runup of 2.9 cm agrees very well with the manual measurement of 2.7 cm at the adjacent 87.5° and

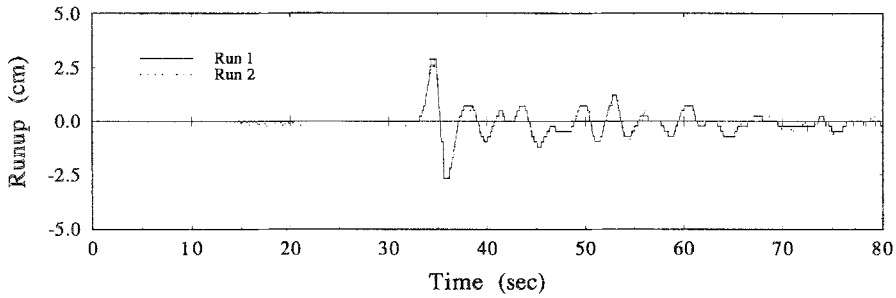

Figure 12
Repeatability for runup time histories for $\mathbf{H} = 0.10$.

Table 6

Comparison of maximum vertical runup

H	m	Test ID	Meas. Ave	Runup Gage
0.05	0.25	5	0.55	0.24
	0.50	6	0.70	0.49
	1	1	0.99	0.97
	2	2	2.00	2.18
	3	3	3.35	3.40
	4	4	4.19	4.37
	0.25*e*	A	—	—
	0.50*e*	B	—	—
	1*e*	7	0.86	0.49
	2*e*	8	1.37	1.21
0.08	0.25	5	0.53	0.49
	0.50	6	0.93	0.73
	1	1	1.91	1.94
	2	2	5.30	5.58
	3	3	9.16	—
	4	4	10.42	10.91
	0.25*e*	A	—	—
	0.50*e*	B	0.23	0.24
	1*e*	7	0.72	0.73
	2*e*	8	2.67	2.91
0.10	0.25	5	0.61	0.49
	0.50	6	1.14	1.21
	1	1	2.67	2.91
	2	2	8.99	—
	3	3	10.53	10.91
	4	4	10.73	10.91
	0.25*e*	A	0.46	0.49
	0.50*e*	B	0.67	0.73
	1*e*	7	1.03	1.21
	2*e*	8	4.04	4.37

92.5° transects (the gage made it impossible to manually measure runup at the 90° transect). The stair-step pattern is due to the resolution of 1 cm (0.24 cm in the vertical) between gage rods. Two runs are overlain, demonstrating excellent repeatability.

Table 6 compares maximum vertical runup between manually measured and runup gage values in centimeters. Measured values are averages of the 87.5° and 92.5° values. Both measured and runup gage values were averaged over two or three runs. In most cases, the agreement is good. The runup gage should read slightly

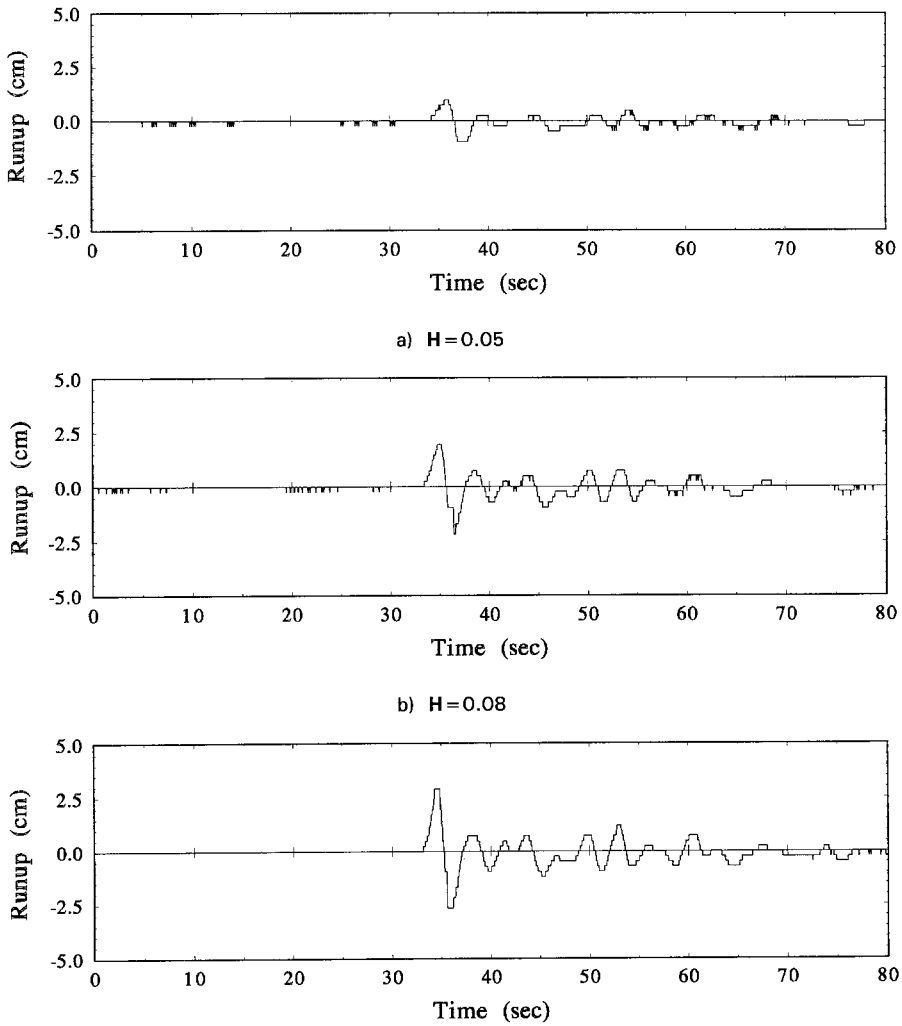

Figure 13
Runup time histories for $m = 1$.

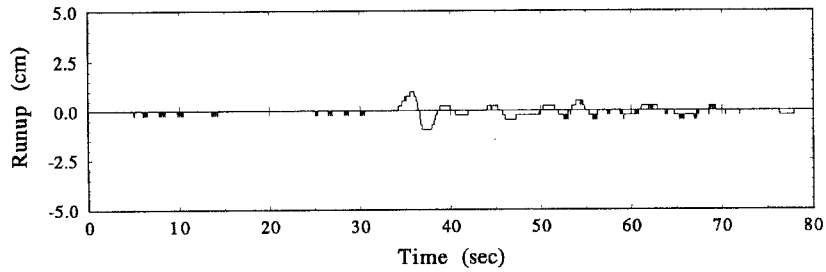

a) m=1

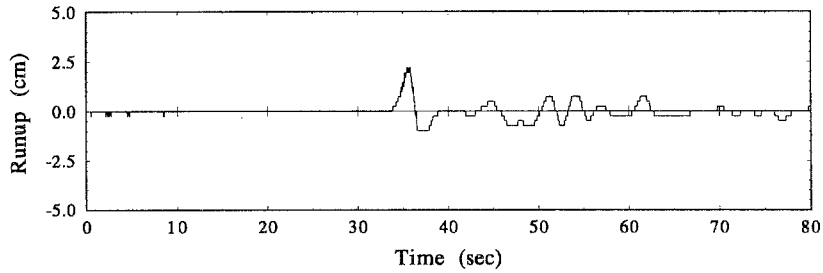

b) m=2

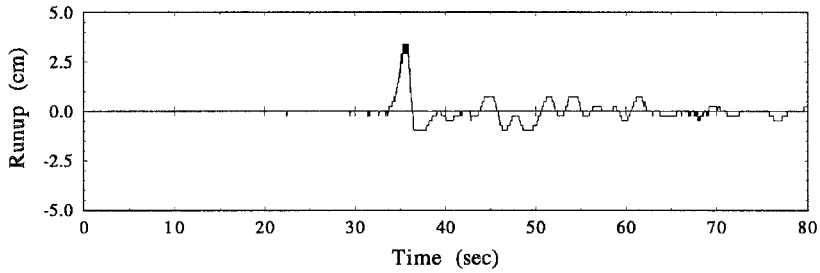

c) m=3

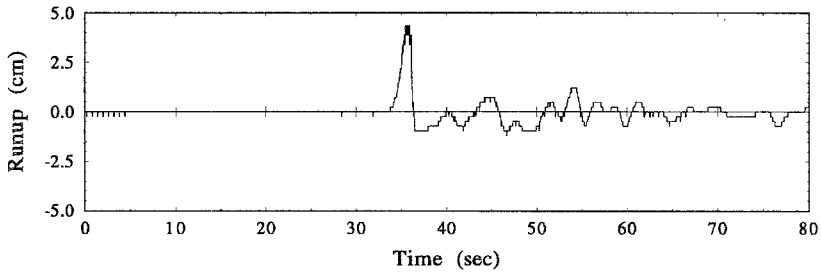

d) m=4

Figure 14
Runup time histories for a range of source lengths at $\mathbf{H} = 0.05$.

higher than the measured values because the gage is over the 90° transect where runup is expected to be the largest. The minimum and maximum runup gage readings were 0.24 and 10.91 cm, respectively. Because of rod spacings of 1 or 2 cm, the resolution varied between ± 0.24 and ± 0.48 cm. In light of this fact, the low readings are within tolerance levels of measured values. Thus, the runup gage is accurate enough to be used in future tests in lieu of manual measurements of maximum runup, a considerable time and cost savings.

Figure 13 shows how the runup time history varies for one symmetric module (i.e., $m = 1$) for a range of wave heights, $\mathbf{H} = 0.05$, 0.08, and 0.10.The amplitude of both the runup and rundown increases as **H** increases. The runup portion appears to increase more than the rundown portion as the number of modules increases (Figure 14) from $m = 1$ to 4 for a fixed $\mathbf{H} = 0.05$.

6. *Summary and Conclusions*

This paper presents results from three-dimensional, laboratory tests of tsunami wave runup on a conical island. The 7.2-m diameter, 62.5-cm tall island had 1 on 4 side slopes and was located in the center of a 30-m-wide by 25-m-long flat-bottom basin. Solitary waves with height-to-depth ratios ranging from 0.05 to 0.20 and "source" lengths ranging from 0.30 to 7.14 island diameters were tested in water depths of 32 cm and 42 cm. Maximum vertical runup measurements were made at 20 locations around the perimeter of the island. Runup on the back side of the island can be higher than the front side, depending on the tsunami wave. Runup time series measurements from a new runup gage show great promise.

Acknowledgements

The authors wish to acknowledge the Office, Chief of Engineers, U.S. Army Corps of Engineers, and the University of Southern California for authorizing publication of this paper. It was prepared as part of the "Three-dimensional Tsunami Runup" study funded by the National Science Foundation through the U.S. Army Engineer Waterways Experiment Station and the University of Southern California (NSF Grants BCS-9205134 and BCS-9201326, respectively). We would especially like to thank the following individuals for their assistance and participation in this project: Mr. David Daily, Mr. Utku Kanoglu, and Mr. Allen Collidge.

REFERENCES

BRIGGS, M. J., and HAMPTON, M. L. (1987), *Directional Spectral Wave Generator Basin Response to Monochromatic Waves*, WES Technical Report, CERC-87-6, USAE Waterways Experiment Station, Vicksburg, MS, 1–90.

BRIGGS, M. J., SYNOLAKIS, C. E., and HUGHES, S. A. (1993), *Laboratory Measurements of Tsunami Runup*, Tsunami '93 Proceedings, Wakayama, Japan, 585–598.

JONSSON, I. G., and SKOVAARD, O. (1979), *A Mild-slope Equation and its Application to Tsunami Calculations*, Marine Geodesy *2*,41–58.

LIU, P.L.-F., CHO, Y.-S., BRIGGS, M. J., and SYNOLAKIS, C. E. (1994), *Runup of Solitary Waves on a Circular Island*, JFM, in revision 1995.

PROVIS, D. G. (1975), *Propagation of Water Waves near an Island*, Ph.D. Thesis, U. Essex.

SMITH, R., and SPRINKS, T. (1975), *Scattering of Surface Waves by a Conical Island*, JFM, *72*, 373–384.

SPRINKS, T., and SMITH, R. (1983), *Scale Effects in a Wave-refraction Experiment*, JFM *129*, 455–471.

SYNOLAKIS, C. E. (1987), *The Runup of Solitary Waves*. JFM *185*, 523–545.

YEH, H., GHAZALI, A., and MARTON, I. (1989), *Experimental Study of Bore Runup*, JFM *206*, 563–578.

YEH, H., IMAMURA, F., SYNOLAKIS, C., TSUJI, Y., LIU, P., and SHI, S. (1993), *The Flores Island Tsunamis*, EOS Transactions, AGU *74*, 33, Aug. 17, 369–373.

YEH, H., LIU, P., BRIGGS, M., and SYNOLAKIS, C. (1994), *Tsunami Catastrophe on Babi Island*, Nature Magazine, November.

(Received September 19, 1994, revised December 29, 1994, accepted January 10, 1995)